SUPERCONDUCTORS, TYPE I AND II

Superconductors differ from normal metals in some truly remarkable ways. In a normal metal, conduction electrons behave as individual particles that move thorough the material, interacting with each other and with the array of ions that

J. Webster (ed.), *Wiley Encyclopedia of Electrical and Electronics Engineering*. Copyright © 1999 John Wiley & Sons, Inc.

form the background lattice. When a voltage is applied, the electrons carry current, scatter randomly, show electrical resistance, and obey Ohm's law. Electrons in a Pb wire at 8 K, for example, will be scattered from impurity atoms and dissipate energy. This electron-scattering process can be modeled by treating the electrons as single particles subject to the Coulomb and exchange forces of the neighboring electrons. The individual-particle picture works well, and one can discuss one electron without concern for the events happening to electrons that are many atomic spacings away.

In a superconducting metal, this individual-particle picture does not hold. Rather, the motion of one electron is highly correlated with other electrons in the metal over very large distances. Again using Pb as an example, when a sample is cooled below the superconducting transition temperature T_c of 7.25 K (1), the electrical resistance drops by more than a factor of 10^{15} in a temperature interval of a few millikelvins. In the course of this transition the motion of the electrons transforms from a single-particle picture to a highly correlated picture. These correlations extend over macroscopic distances and the electrical resistance vanishes. During the superconducting transition, the wave function of the electrons develops a certain rigidity, and the electrons tend to move as a giant molecule rather than as individual particles.

This rigidity is reflected in a special feature of superconductivity called *phase locking.* Electrons, like all elementary particles, have both a particle and a wave character and the wave properties are described by a wave function $\psi = Ae^{i\phi}$ with both an amplitude A and a phase ϕ. In the course of the superconducting transition, the phase ϕ of any one superfluid electron becomes tightly locked to the phase of all the neighboring superfluid electrons. This rigidity and phase locking of the wave function leads to most of the remarkable properties of superconductors. It leads to the suppression of scattering, to zero electrical resistance, to the expulsion of magnetic flux from the interior of a superconductor, and to all of the marvelous aspects of quantum interference effects that are so crucial to microelectronic devices. It is important to understand how this rigidity and phase locking come about.

There are two very broad classes of superconductors that are distinguished from one another by the way magnetic flux is distributed inside the material. In one class, called type I, the magnetic flux is totally excluded from the interior of a bulk sample, and the magnetic induction B is zero everywhere except for a thin layer that is a few hundred nanometers thick near the surface. This thin layer is called the penetration depth λ, and the $B = 0$ state is called the Meissner state. In this thin layer, surface currents flow to cancel the applied field and give $B = 0$ in the interior. It is useful to recall here that B in the interior is the sum of the applied field, $\mu_0 H$, plus the field due to circulating currents in the material, $\mu_0 M$, where H is the magnetic field and M is the volume magnetization. When the external magnetic field reaches a certain critical magnitude called the thermodynamic critical field H_c, the superconducting state collapses and the material reverts to the normal state at higher fields. This is illustrated by the dashed curve in Fig. 1.

In the second class of materials called type II, as you increase the magnetic field from zero, the flux is totally excluded at first, just as for type I material. Then, at some characteristic field called H_{c1}, the magnetic flux begins to enter the material in the form of tiny vortices of magnetic flux, called flux quanta Φ_0. Each quantum carries 2.07×10^{-15} Wb of magnetic flux. With further increases in H, the quantized vortices flood into the material until an upper critical field, H_{c2}, is reached where the sample again reverts to the normal state. These lower and upper critical fields are illustrated on the diamond points of Fig. 1.

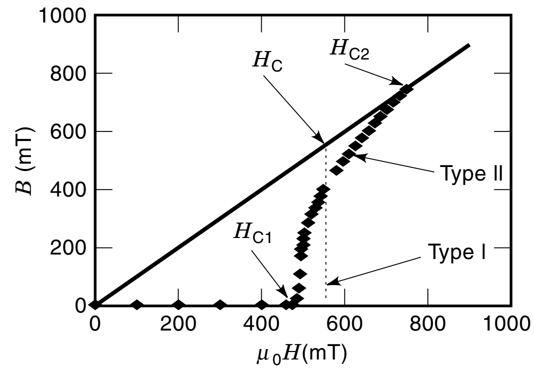

Figure 1. B vs $\mu_0 H$ plot to illustrate the defining characteristics of type I and type II superconductors.

The purpose of this article is to review the microscopic origins of these two types of magnetic behavior for superconductors. We will discuss the features that distinguish type I from type II materials, and describe the way in which type I materials can be transformed into type II materials by alloying. Discussion will include both the classical superconductors and the cuprate superconductors that were discovered in 1986 (2) to have extraordinarily high T_c. After taking a brief look at a few typical examples of type I and type II behavior, we will review some features of the superconducting wave function that leads to the remarkable properties of superconductors. Then we will return to a more detailed discussion of more subtle aspects of type I and type II behavior. Various practical methods to measure the characteristic fields of H_c, H_{c1}, and H_{c2} will be explored. Throughout, there will be an attempt to provide useful equations for computation, even though the derivation of the relations is beyond the scope of this presentation. The goal here is to discuss the behavior of these two classes of superconductors using simple physical pictures wherever possible.

TYPICAL EXAMPLES

Superconductivity is a very common phenomenon. Approximately half the elements in the periodic table and a large number of intermetallic compounds show the effect. Often, it is necessary to go to rather low temperatures and in some cases it is necessary to apply high pressure to transform the material into a superconductor. Although there are exceptions, pure elemental metals tend to be type I superconductors and alloys tend to be type II superconductors.

Low-T_c Type I Superconductors

In many classical superconductors, such as high-purity Pb, Hg, and In (1,3), the magnetization curves, M versus H, exhibit a Meissner ($B = 0$) behavior up to some critical field at which the magnetic flux suddenly collapses into the sample

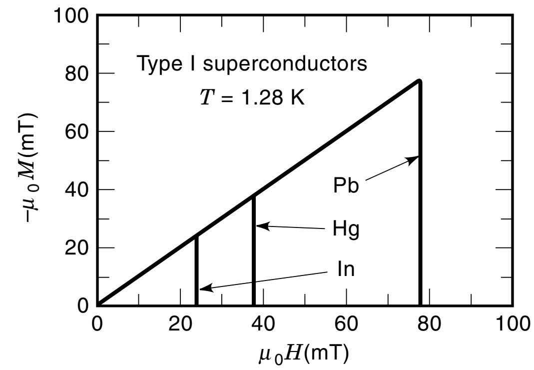

Figure 2. Magnetization curves for Pb, Hg, and In at 1.28 K showing typical values of H_c.

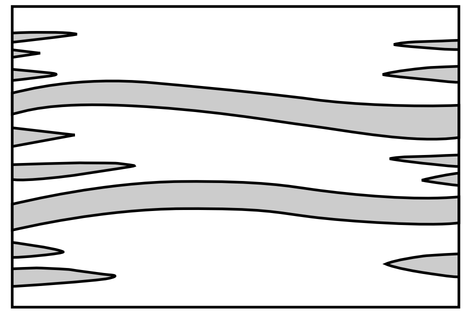

Figure 4. A typical magnetic flux distribution in the intermediate state of a type I superconductor as lamella of normal-state regions (shaded area) collapse into the interior. This is for a flat plate with H perpendicular to the plate.

as shown in Fig. 2 for 1.28 K data. Generally speaking, very pure metals that have s-band or p-band conduction electrons at the Fermi surface will show this so-called type I behavior. Very pure metals that have a relatively high Fermi velocity v_F and a relatively low T_c tend to be type I superconductors.

A more detailed look at the magnetization curves reveals that the collapse of flux into a bulk sample occurs over a finite magnetic field interval. When the flux begins to enter the sample, the slope of the line is governed by demagnetizing effects (4), that is, effects associated with the shape of the sample. As shown in Fig. 3, a magnetic field applied to a superconductor in the Meissner state has a larger field at the "equator" of the ellipse than the applied field H_a. For this elliptical sample, flux begins to enter the sample at $H_a = (1 - \delta)H_c$ and the transition is complete at H_c. δ is called the demagnetizing factor. Because the free-energy difference between the superconducting and normal state is directly related to H_c, it is called the thermodynamic critical field curve.

Intermediate State

Between $(1 - \delta)H_c$ and H_c, the material breaks up into an intermediate state in which both Meissner regions and normal regions coexist in the sample. When the screening currents that are flowing in the penetration depth region near the surface reach a critical value, normal regions will nucleate at the surface and propagate into the interior of the sample. Usually this happens when the kinetic energy of the electrons in the circulating screening current are a significant fraction of characteristic superconducting energy, $k_B T_c$. Here, k_B is the Boltzmann constant. The detailed shape of the Meissner regions in the intermediate state depends on structure of the material and the shape of the sample. Normal regions nucleate at the surface and often propagate into the interior in the form of lamellar regions as shown in Fig. 4. For a long slender sample with the magnetic field parallel to the long axis of the sample, δ is close to zero and the region of the intermediate state is narrow. This behavior is illustrated by the data in Fig. 2. For a sphere, δ is $\frac{1}{3}$, and the magnetization curve is illustrated in Fig. 3. For a flat plate with the magnetic field perpendicular to the plane of the plate, δ is close to 1, and the sample enters the intermediate state at fields far below H_c. Shoenberg, p. 103 (5), gives a detailed discussion of the intermediate state for spheres and Tinkham, p. 25 (6), gives a detailed discussion for flat slabs.

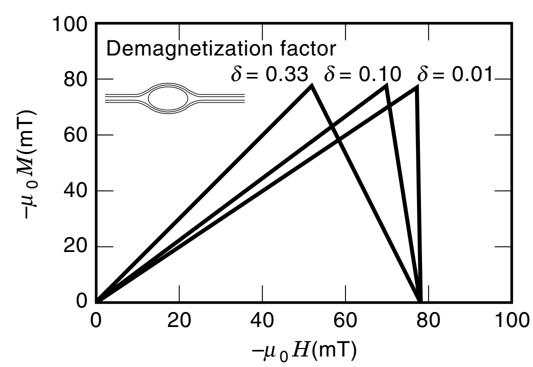

Figure 3. Change in the shape of the magnetization curves for a given material as the demagnetizing factor increases. The inset shows an elliptical sample in the Meissner state with the field at the equator larger than the applied field.

Low-T_c Type II Superconductors and the Vortex State

Magnetization curves for three different transition metals are shown in Fig. 5. Very pure Ta is a type I material (7) with an abrupt collapse of the superconducting state similar to Pb. The other two very pure transition metals, Nb and V, show a much broader transition to the normal state and are called type II superconductors (8,9). When very pure metals show type II behavior, they are called intrinsic type II superconduc-

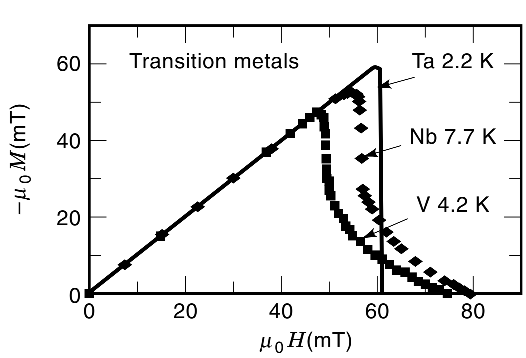

Figure 5. Magnetization curves for three transition metals to illustrate both type I (Ta) and type II (Nb and V) behavior.

tors. The interval between H_{c1} and H_{c2} is called the vortex state because in this magnetic field interval, the sample fills with vortices, each carrying one quantum of flux, Φ_0. In all of these intrinsic type II materials, the conduction electrons at the Fermi surface are mostly d band in character, so the Fermi velocity is relatively low. In addition, T_c is relatively high. The magnetization data in three samples shown here are highly reversible, and therefore the first flux entry is very close to the field at which a vortex is thermodynamically stable in the material, H_{c1}. For the data shown in Fig. 5, a temperature is chosen so that H_c is in the vicinity of 50 to 60 mT. This permits an easy comparison of the shapes of the curves. As the temperature is decreased, the ratio of H_{c2}/H_c typically rises by about 50%, and the slope of the magnetization at H_{c2} always decreases. Among the transition metals, very pure Ta (9) is an exception in that it is type I. A very small amount of impurity, however, will transform it to a type II material very similar to Nb and V.

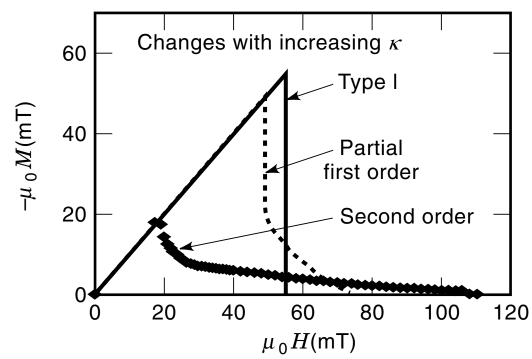

Figure 6. Transformation from type I to type II behavior as l is gradually increased. For κ just greater than 0.707, there is an attractive interaction between vortices and a first-order transition at H_{c1}. This illustrates the change in shape of magnetization curves as impurities are added.

Low-T_c Alloys

To understand the difference between type I and type II superconductors on a microscopic scale, it is essential to know that there is a characteristic distance, called the coherence distance, ξ, over which the superconducting wave function can change. In a superconductor, the basic charge-carrying unit in the system is a highly correlated pair of electrons called the Cooper pair. The minimum distance in which the density of superconducting electrons, n_s, can change from the value in the bulk superconductor to zero in a normal metal is roughly the size of these Cooper pairs. The coherence distance, or the size of the Cooper pairs, is a very important property of a superconductor and typically varies from about 1 μm in Al to as small as 2 nm in the cuprate superconductors. In the transition metals such as Nb and V $\xi \sim 30$ nm and in the conventional type I materials such as Sn, Pb, Hg, and In $\xi \sim 500$ nm.

The critical factor governing the shape of the magnetization curves of superconductors is the ratio of the magnetic field penetration depth to the coherence distance, λ/ξ. This ratio is sufficiently important that it is given a symbol of its own,

$$\kappa \approx \lambda/\xi \tag{1}$$

Small-κ materials are type I, and large-κ materials are called type II. The transition from type I to type II behavior occurs at $\kappa \approx 1/\sqrt{2} = 0.707$. In a type I superconductor, H_c is directly related to the free-energy difference between the superconducting and normal state by the area under the magnetization curve,

$$G_n - G_s = -\int_0^{H_c} \mu_0 M dH = \mu_0 H_c^2/2 \tag{2}$$

In type II materials, H_c retains this definition. The ratio κ from Eq. (1) also is related to the characteristic critical fields on the magnetization curve via

$$\kappa = H_{c2}/\sqrt{2}H_c \tag{3}$$

The range of the correlations among the electrons and hence ξ in a superconductor can be reduced by shortening the normal-state mean free path of the electrons, l. Hence, one should expect that alloying would reduce both l and ξ and would cause a transition from type I to type II behavior if λ remains roughly constant. This was shown to be true, for example, by Kumpf (10), who demonstrated that pure Pb with $\kappa \sim 0.4$ could be converted to a type II material with $\kappa \sim 0.84$ with the addition of 2.0 at. % Tl. For this Pb system, it requires a resistivity of $\rho_n \sim 2\ \mu\Omega \cdot$cm to change Pb from a type I to a type II superconductor. To convert pure Ta from type I to type II, it requires alloying until $\rho_n \sim 0.5\ \mu\Omega \cdot$cm.

The sketch in Fig. 6 shows the changes that occur in the magnetization curves as κ is gradually increased for a material similar to Ta. For κ substantially less than 0.707, the magnetization curves are typical type I with a complete first-order transition to the normal state at H_c. A first-order transition has a latent heat, but a second-order transition has no latent heat. For κ comparable to $1/\sqrt{2}$, there is a partial first-order transition at H_{c1} with a tail in the magnetization extending out to H_{c2} as shown by the dashed line in Fig. 6. For κ substantially larger than $\sqrt{2}$, the phase transition is second order at H_{c1}. As shown by Auer and Ullmaier (7), the range of κ showing the type II behavior with a first-order transition at H_{c1} depends on temperature. Figure 7 is a sketch showing roughly the expected behavior. The horizontal line on Fig. 7 is $\kappa = 1/\sqrt{2}$.

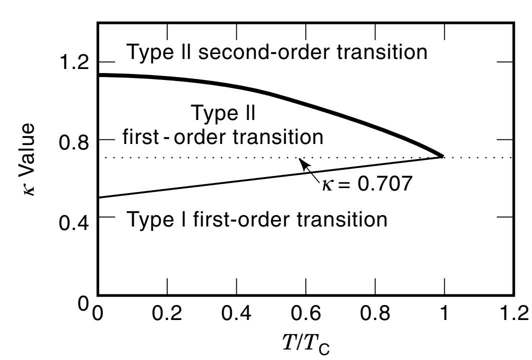

Figure 7. The transformation from type I to type II behavior on a κ vs. T plot. This qualitatively shows the boundaries of these three different types of phase transitions.

Because l is closely connected to the normal-state resistivity ρ_n, κ can be related to ρ_n and the κ value for the pure metal, κ_0, by the useful relation

$$\kappa = \kappa_0 + 7.5 \times 10^5 \gamma^{1/2} \rho_n \tag{4}$$

where γ is the electronic specific constant and ρ_n is the resistivity. If you use units where γ is in erg/cm$^3 \cdot$ K^2 and ρ_n is in $\Omega \cdot$ cm, then the constant is 7.5×10^3. For the extreme dirty or short mean-free-path limit, Hake (11) showed that Ti–16 at. %Mo samples with $\rho \sim 100\ \mu\Omega \cdot$ cm can be nearly reversible with a κ value of 66.

Among the high-purity *s-p* band metals, κ ranges from 0.01 for Al, to 0.15 for Sn, to 0.4 for Pb. Among the high-purity transition-metal superconductors, κ ranges from 0.36 for Ta, to 0.78 for Nb, to 0.90 for V. Nitrogen impurities are particularly good to show the transition from type I to type II behavior because they go into the lattice of Ta as statistically distributed interstitial atoms. Hence, N decreases the electronic mean free path without forming clusters that would substantially increase the pinning of vortices and irreversibility effects. As shown by Auer and Ullmaier (7), Ta is transformed from a type I to a type II superconductor when the sample residual resistivity $\rho_0 = 585\ \mu\Omega \cdot$ cm and attains a κ value of about 1.5 when $\rho_0 \sim 2000\ \mu\Omega \cdot$ cm.

High-T_c Materials

The high-temperature superconductors (HTS) such as $La_{1.85}Sr_{0.15}CuO_4$, La(214), are qualitatively different from all of the metals that had been studied before. They are different because the normal state is created by doping an insulator. They also are different because they tend to be rather anisotropic with the charge carriers moving most easily in the *a-b* planes of the CuO_2 sheets. The parent cuprate for La(214) with no Sr doping, $La_2Cu_1O_4$ is not a superconductor and is not a metal. Rather, it is an antiferromagnetic insulator. If, however, part of the trivalent La ions are replaced by divalent Sr ions, holes are created in the copper oxide planes and the material becomes an anisotropic normal metal and a superconductor with T_c of about 42 K. In these oxide conductors, the carrier mobility along the copper oxide planes is much higher than it is perpendicular to the copper oxide planes, so both the normal conductivity and the superconductivity are quite anisotropic.

In the superconducting state, the magnetization data for the cuprate superconductors show type II behavior with very high κ values, commonly about $\kappa \sim 100$. Hence, H_{c2} is over 100 times larger than H_c. For many of these cuprates, the penetration depth is about 200 nm, and the coherence distance along the copper oxide planes is about 2 nm. Along the c axis, the coherence distance is even smaller at ~0.5 nm.

PHYSICAL PICTURES FOR TYPE I AND TYPE II PHENOMENA

Superconductivity is rather special in the field of condensed-matter physics because it is a manifestation of quantum mechanics on a macroscopic scale. If one induces a supercurrent to flow in a superconducting ring, the circulating charge carriers obey the Bohr-Sommerfeld quantization condition even if the diameter of the ring is hundreds of micrometers. In a single atom, such as the hydrogen atom, the angular momentum of the circulating electron is quantized because the wave function of the electron must be single valued going around the atom by 2π. This quantization of angular momentum in the hydrogen atom is then reflected in a quantization of the magnetic moment in units of Bohr magnetons. The same kind of quantization occurs for superconducting electrons circulating in a large ring. Because the electrons are phase locked, the wave function must be single valued and the Bohr-Sommerfeld quantization condition, $\int p dq = n\hbar$, is obeyed. Here, p is the momentum, dq is the path element, and n is an integer. This creates quantized circulating currents, and the resulting flux also is quantized in units of $\Phi_0 = h/2e$.

Even though quantum mechanics is fundamental to understanding superconductivity, there are some simple pictures that enable the beginner to visualize where the electrons or holes are and how they interact. The goal of this section is to present some of the vocabulary and ideas of the Bardeen-Cooper-Schrieffer (BCS) (12) theory in a way that one can picture the basic behavior of type I and type II superconductors.

Idea 1: All Superconductors Look Alike

There is a great deal of similarity in the physical properties of superconductors. If the thermodynamic critical field is plotted as a function of temperature or the superconducting energy gap in the excitation spectrum, Δ, as a function of temperature, the curves have the same functional form and the values scale with the transition temperature. The ratio of $H_c(T = 0)/T_c$ is always about 10 mT/K, and the ratio of $\Delta(T = 0)/k_B T_c \sim 1.8$ for the low T_c superconductors. Because superconductors are so similar, there is a reasonable expectation that the details of the metal are not terribly important in the basic explanation of superconductivity. A rather general and simple theory may explain the effect.

Idea 2: BCS Theory

In the development of a theory of superconductivity, BCS constructed the superconducting ground state by taking special combinations of normal-state wave functions. At the superconducting transition, the space dependence of the wave functions do not change, but rather the occupation probability of a given state changes. To create the superconducting wave function, the electrons are allowed to exchange phonons, thus scattering around the Fermi surface and coherently mixing the normal-state wave functions. Instead of the random occupation of states at the Fermi surface that occurs in a normal metal, the system can gain energy via phonon exchange if the electronic states are occupied in pairs. This pairing increases the amount of phonon exchange that can occur and each phonon exchange lowers the energy a bit. To define terms more explicitly, pair occupation means that if the state with momentum $\hbar k$ is occupied, then the state with momentum $-\hbar k$ also is occupied. Similarly, if the state with $\hbar k$ is empty, then the state with $-\hbar k$ also is empty. The pairs are chosen to have equal and opposite momentum because, by symmetry, this choice gives the maximum number of final states for the electron-phonon scattering and maximizes the phonon exchange. As the metal undergoes the superconducting transition, it is the probability of occupation that changes. It changes from a random occupation to a pair occupation.

In BCS theory, three essential variables are used. First, the normal-state density of states at the Fermi surface, $N(0)$, is a measure of the number of electrons participating. The number of electrons that can take advantage of phonon exchange is determined by $N(0)$. Second, the Debye energy $\hbar\omega_D$ is a measure of the range of phonons available for the electron-phonon exchange process. Third, the strength of the electron-phonon interaction, V, is a measure of the amount of energy the electrons gain in a phonon exchange. Within the theory, the superconducting transition temperature T_c will be calculated to be

$$k_B T_c \approx \hbar\omega_D e^{-1/N(0)V} \tag{5}$$

This provides a connection between the transition temperature and the three variables in the theory. If, in addition, one works out the minimum energy to create an excitation out of the superfluid ground state by disrupting one pair of electrons, at $T = 0$, this turns out to be

$$\Delta_0 \approx 1.8 k_B T_c \tag{6}$$

Disrupting a pair simply means preventing that pair of states from participating in the coherent phonon exchange. This minimum energy to create an excitation in a superconductor, Δ, is often called the order parameter or the energy gap, and typically it is about 1 meV for a T_c of 7 K. The value of Δ decreases from the $T = 0$ value, Δ_0, as the temperature rises and goes to zero at T_c. Our goal here is to provide a physical picture to go with these equations.

Idea 3: The Cooper-Pair Problem

A first step in the development of the BCS theory was the Cooper-pair problem (13). Cooper showed that there is a fundamental instability in an electron gas if one introduces an attractive interaction that scatters electrons around the Fermi surface. In this problem, you start with one pair of electrons outside a Fermi sea. Without the electron–phonon interaction, the energies available to the electrons are the usual free-electron energies above the Fermi energy E_F, as shown by the dotted lines in Fig. 8. The solid horizontal lines are filled states below the Fermi sea. When the electron–phonon interaction is introduced, the new energies for the perturbed

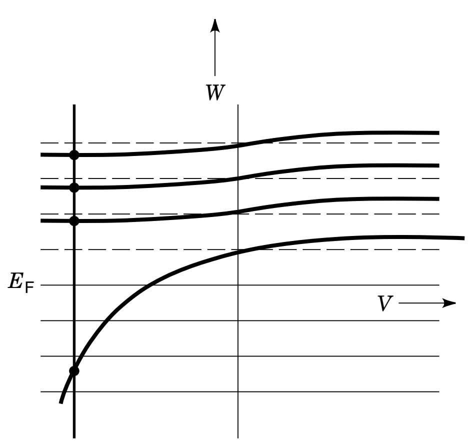

Figure 8. Energy-level diagram for the Cooper-pair problem. Here W is the new energy of the pair state and V is the strength of the perturbing interaction. Note that for large and negative V, one state falls far below the Fermi energy.

system, W, are represented by the heavy solid lines. Here they are plotted as a function of the strength of the interaction, V. Note that if V is positive or repulsive, all the energies are pushed up a bit above the unperturbed dotted line values. Note also that if V is negative or attractive, all of the energies are pushed down a bit except the level just above E_F. This level is pushed far below E_F. The splitoff of this state far below E_F means that a free-electron gas with random occupation of states is unstable to the formation of pairs when an attractive interaction is introduced. The energetically most favored combination of electrons for this phonon exchange occurs when the pair has zero center-of-mass momentum (electrons have equal and opposite momentum), hence, giving the lowest energy. Experiments have shown that the pairs of electrons also are known to have opposite spin. Presumably this antiparallel spin arrangement arises from a quantum-mechanical effect called exchange forces. Electrons with opposite spins are closer together than electrons with parallel spins so they can take better advantage of the electron–phonon interaction. Hence, pairs with opposite spin and momentum have the lower energy. If some other type of interaction were to cause pairing, then a parallel spin arrangement is possible.

A special feature of the Cooper pair problem is that the normal-state wave functions that are being mixed by the electron–phonon interaction all add in phase at some point in real space to form a wave packet. This packet is the so-called Cooper pair and by the summation of occupied states, it has a real-space extent of the coherence distance,

$$\xi = \hbar v_F/\pi\Delta_0 = 0.18\hbar v_F/k_B T_c \tag{7}$$

Equation (7) shows that the coherence distance, or the size of the Cooper pairs, is directly related to the ratio of v_F/T_c. Because the *s-p* band metals tend to have relatively high v_F and low T_c, they would be expected to have large coherence distances and hence tend to be type I superconductors. The basic charge-carrying unit in the circulating current around a superconducting vortex in a type II material in the vortex state is the Cooper pair.

Idea 4: BCS Theory and Pair-Pair Correlations

The Cooper-pair problem is only part of the picture because it describes just one pair of electrons outside a Fermi sea. The total problem must deal with all of the electrons and must deal with their correlated motion. If typical numbers are put into Eq. (7), Al has $\xi \sim 1600$ nm, Sn has $\xi \sim 230$ nm, Pb has $\xi \sim 83$ nm, and Nb has $\xi \sim 40$ nm. Given the normal density of electrons in a metal, there are thousands to millions of pairs occupying the space of any single pair. Hence there is a great deal of pair-pair overlap. These highly interacting and overlapping Cooper pairs provide a physical picture for the origin of phase locking over macroscopic distances.

The high-temperature superconductors are a very special case because the coherence distance is so short. Typically, $\xi \sim 2$ nm so the overlap of Cooper pairs is much less in this class of materials and the phase locking is less strong. For HTS, the number of pairs overlapping any one pair is measured in dozens rather than thousands to millions. This leads to a less rigid vortex lattice and a greater susceptibility to flux creep.

The BCS problem is similar in some ways to a variational calculation in an undergraduate quantum-mechanics course.

One guesses a form for the wave function with the pair occupation number as an adjustable parameter. Next one writes an expression for the free energy of the system in terms of this trial wave function and minimizes the energy as a function of pair occupation. In both the Cooper and BCS problems, a paired trial wave function is selected in order to maximize the final states available for electron-phonon scattering. One result of the theory is that it is energetically favorable to mix normal-state wave functions within an energy band that is Δ wide near E_F. All of the pairs share the same states so there is an energy advantage for correlated motion of many pairs to make most efficient use of the states available for electron-phonon exchange. Pair-pair correlations are critical because they provide the fundamental mechanism to propagate phase coherence over long distances.

To create an excitation from the superconducting ground state, one of the pair states is simply disrupted. If a pair state is broken, say by injecting an electron into one of the two states of a pair in the metal, then other pairs cannot use that channel for phonon exchange. That pair state is removed from the coherent phonon exchange for all of the other electrons. This raises the energy of all the electrons in the ground state. In computing the ground-state energy and the excitation energies, one has to give up the single-particle picture and go to a highly correlated many-paired electron picture in which the disruption of one pair changes the energy of all the pairs in the ground state.

Idea 5: Phase Locking and Rigidity of the Wave Function

A central feature of superconductivity is that the electrons phase lock into a many-electron ground-state wave function that has a substantial amount of rigidity. If the system is disturbed, it responds as a giant unit rather than responding as individual particles. In the Cooper problem, a pair of electrons is formed by mixing normal-state wave functions so that they all add in phase at some point in space. In the BCS problem, pair-pair correlations play a central role because all of the pairs are using the same states for electron-phonon scattering. This leads to a highly correlated ground-state superfluid that extends over macroscopic distances. The ground state is somewhat like a giant macromolecule in that the superfluid is phase locked and responds as a rigid unit. A common analog in chemistry would be a benzene molecule in which the electrons in this benzene ring respond as a rigid unit to small stimuli. In a superconducting Pb wire 1 m long, the electrons at one end are phase locked to the electrons at the other end.

Pairs, of course, can be disrupted by many processes: by thermal (k_BT) excitations, by electromagnetic absorption, or by electron injection. In all of these cases the disrupted electrons or excitations behave just like normal-state electrons. The ground-state electrons can be thought of as a superfluid with density n_s, with a condensation energy or pairing energy Δ per pair. The excitations out of the ground state can be thought of as a normal fluid with density n_n. In this framework the sum of these probabilities must add to one, $n_s + n_n = 1$. This picture is quite analogous to the two-fluid model originally proposed by London (14). As the temperature rises, the incoherent phonon scattering becomes larger and overwhelms the coherent phonon exchange and the material reverts to the normal state.

Zero Electrical Resistance

Electrical resistance in a material such as Pb disappears below the superconducting transition temperature because a significant fraction of the electrons transform into a coherent, phase-locked, superfluid ground state having considerable rigidity in the wave function. In a normal metal, such as Pb above T_c, the electrons are relatively uncorrelated and behave as individual particles. Electrical resistance arises because individual electrons scatter from impurity atoms, phonons, or some other excitation in the metal as random or thermal events. In a superconductor, electrons are locked together in a giant rigid wave function and individual scattering is essentially eliminated. The reason that the transition is so sharp is that there is such overkill in the pair-pair correlation. With millions of pairs overlapping the region of any one pair, one can get substantial pair-pair correlation even if only 0.1% of the electrons are in the superfluid state. This can occur within a temperature interval of a millikelvin.

Meissner Flux Exclusion in Type I Materials

In thinking about the ability of a type I superconductor to push magnetic flux out of the interior to give $B = 0$, it is important to remember that the free-energy difference per atom to push the flux out is very small. The value of $G_n - G_s$ given by Eq. (2) can be evaluated to be about 10^{-8} eV per atom. This is tiny compared with most electronic processes, which are about 1 eV. Hence, it does not take much energy to exclude the flux.

There are several competing energies in this problem. If a magnetic field penetrates the interior of a sample where the paired superfluid density is high, then there is a tendency for the spins to align with the field and thus break pairs. This would raise the free energy. This rise in free energy would be prevented if circulating currents are created at the surface of the sample to cancel the magnetic field to give $B = 0$. There is, of course, a kinetic energy cost in creating these circulating supercurrents. For small κ and $H < H_{c1}$, it is energetically more favorable for the material to develop a supercurrent at the surface and provide a $B = 0$ condition in the interior than it is to lose the condensation energy associated with breaking pairs as the spins align with the applied magnetic field. If, however, κ is greater than $1/\sqrt{2}$ and $H > H_{c1}$, it is energetically favorable for quantized vortices to enter the material.

The time dependence of the response of the electrons to an applied magnetic field is governed by the plasma frequency. With the application of an external field, the superconducting electrons respond as a coherent plasma, and the screening length for magnetic fields is given by

$$\lambda^2 = m^*/\mu_0 n_s e^2 \qquad (8)$$

where m^* is an effective mass and e is the charge on the electron. For very pure metals, $\lambda \sim 50$ nm and for the HTS materials, $\lambda \sim 170$ nm. Because λ is governed by the superfluid density, it does not vary from superconductor to superconductor as strongly as ξ, which is governed by the ratio of $\hbar v_F/k_BT_c$.

Ginzburg–Landau Equations

Very early in the development of the theory of superconductivity, Ginzburg and Landau (15) developed a very general and yet very powerful formulation of the problem. They assumed that there is an order parameter that behaves much like a wave function, and they further assumed that this wave function ψ is related to the local density of superconducting electrons by $|\psi|^2 \sim n_s$. The free energy is then written as the sum of a kinetic energy term, a potential energy term, and a magnetic term:

$$G_s - G_n = \frac{1}{2m}\left|\left(\frac{\hbar}{i}\nabla - eA\right)\psi\right|^2 + \alpha|\psi|^2 + \frac{\beta}{2}|\psi|^4 + \frac{h^2}{8\pi} \quad (9)$$

Here, the potential energy term is a power-series expansion in $|\psi|^2$ and $h^2/8\pi$ is the magnetic energy term. Minimizing this free energy with respect to the order parameter gives the famous Ginzburg–Landau (GL) equation:

$$\alpha\psi + \beta|\psi|^2\psi + \frac{1}{2m^*}\left(\frac{\hbar}{i}\nabla - eA\right)^2\psi = 0 \quad (10)$$

Excellent discussions of solutions of these equations are given by Fetter and Hohenberg (16), Tinkham (6), and de Gennes (17).

A central factor determining whether a material is a type I or type II superconductor is the boundary energy between a superconducting region and a normal region. If a superconductor–normal-metal boundary has a positive surface energy, then the system will minimize the boundary area and a Meissner solution will be expected. If the superconductor–normal-metal boundary has a negative surface energy, then it will be expected that the material will be unstable against a breakup into small domains in order to maximize the amount of superconductor–normal-metal boundary area. In the original paper (15), it was shown by numerical calculations that for Eq. (10), the onset of negative surface energy occurs when the ratio of two characteristic lengths, the penetration depth and the coherence distance, is equal to 0.707 or

$$\kappa \approx 1/\sqrt{2} \quad (11)$$

This criterion then specifies whether a superconductor is type I or type II.

Vortex State

Building on the GL result, Abrikosov (18) predicted in 1957 that flux entering a type II superconductor is in the form of quantized vortices. A quantized vortex with Φ_0 of flux is the minimum unit of flux that can enter. He showed that if $\kappa > 1/\sqrt{2}$, then a regular array of flux tubes or vortices would form in the interior of the material. The stable state is a triangular array so the area of a flux tube would be

$$\frac{\sqrt{3}}{2}a_0^2 = \frac{\Phi_0}{B} \quad (12)$$

where a_0 is the lattice spacing of the triangular lattice. More detailed calculation shows that vortices are first stable in a superconductor at

$$H_{c1} = \frac{H_c}{\sqrt{2}\kappa}\ln\kappa \quad (13)$$

If there are no surface barriers to flux entry, vortices will nucleate and move into the interior above H_{c1}. As the applied field increases, the vortices crowd closer together. At high magnetic field, when the cores of the vortices begin to overlap, the sample goes normal. This occurs at

$$H_{c2} = \frac{\Phi_0}{2\pi\xi^2} = \sqrt{2}\kappa H_c \quad (14)$$

Combining Eq. (13) with Eq. (14) gives a convenient rule of thumb that $H_{c1}H_{c2} \approx H_c^2 \ln \kappa$.

Large-κ Case: Repulsive Interaction Between Vortices

For the case of $\kappa \gg 1/\sqrt{2}$, the Ginsburg–Landau equations have relatively simple solutions and there are rather good physical pictures to describe the behavior of vortices. A reasonably good model to describe the vortex is a normal core of radius ξ with circulating currents sufficient to give one quantum, Φ_0, of flux. The superconducting order parameter Δ is zero in the center of the core and rises toward the bulk value with a characteristic length ξ. To estimate the free energy per unit length of the vortex, g_v, the free energy per unit volume, $\mu_0H_c^2/2$, can be multiplied by the area of the core, $\pi\xi^2$. A more accurate calculation (6) gives

$$g_v \approx (\mu_0 H_c^2/2)(4\pi\xi^2)\ln\kappa \quad (15)$$

The magnetic field around the vortex is given by (6)

$$h(r) = \frac{\Phi_0}{2\pi\lambda^2}K_0(r/\lambda) \quad (16)$$

where K_0 is the zeroth-order Hankel function of imaginary argument. The force on a quantized vortex in the presence of a current density J is (6)

$$f_p = J\Phi_0 \quad (17)$$

where J can be either the current density caused by the circulating current of other vortices or a transport current density that is externally applied. In this large-κ regime, the force between vortices is repulsive and the Abrikosov theory (18) shows that the vortices will arrange themselves in a triangular array. As the field rises above H_{c1}, the vortices flow into the interior under the influence of the magnetic pressure of the applied field.

The high-T_c cuprate superconductors normally have a coherence distance in the a-b plane on the order of $\xi_{ab} \sim 2$ nm and a penetration depth on the order of $\lambda \sim 200$ nm so the κ values are in the range of $\kappa \sim 100$. In this extreme type II limit, the size of the Cooper pairs is very small compared to the vortex size and several simplifying assumptions can be made in the development of models to describe the magnetization curves.

The Hao and Clem model (19) for the magnetization curves of high-T_c superconductors is typical of approaches that can be used. They developed a variational method in which the trial wave function is written as

$$\psi = \frac{\rho}{\sqrt{\rho^2 + \xi_0^2}}\psi_\infty \quad (18)$$

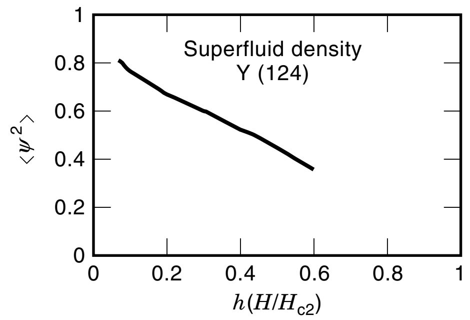

Figure 9. Superfluid density as a function of magnetic field for Y(123). These data show that the superfluid density falls linearly with magnetic field and approaches zero as H goes to H_{c2}.

where ρ is the distance from the core of the vortex, and both ξ_v and ψ_∞ are adjustable variables in the trial wave function. They start with the free energy including the core energy and minimize with respect to the trial variables of ξ_v and ψ_∞. The magnetization curves are found to scale to a universal function on a $\mu_0 M/\sqrt{2}H_c$ vs $H/\sqrt{2}H_c$ plot. Both $Y_1Ba_2Cu_3O_{7-\delta}$ and $Y_1Ba_2Cu_4O_{8-\delta}$ are found to obey the Hao-Clem model very well (19). In addition, it was found that the superfluid density averaged over one vortex unit cell falls linearly as H/H_{c2} for fields greater than $0.3H_{c2}$ over the entire range where there is thermodynamic reversibility and measurements can be made (20). Figure 9 shows that $n_s \sim |\psi|^2$ is linear in H/H_{c2} for this high-T_c Y(123) material.

Surface Superconductivity

The surface of the superconductor modifies the potential for the superfluid electrons, and superconductivity will persist to fields above H_{c2} in a narrow layer near the surface. With the applied field parallel to the flat surface (17), Ginzburg-Landau theory with plane surface boundary conditions predicts that a superconducting layer about a coherence distance thick will be present up to $H_{c3} = 1.7H_{c2}$. Experiment verifies that this basic idea is correct. For the case of pure Nb, the measured ratio of H_{c3}/H_{c2} for pure Nb varies from 1.78 at low temperatures to 1.70 at $T/T_c = 0.9$ (21). At higher temperatures, H_{c3}/H_{c2} approaches 1.0 at T_c. Altering of the surface condition, say, by a normal metal coating will suppress or destroy this surface state.

Small-κ Case: Attractive Interaction Between Vortices

For the case in which ξ is comparable to λ, there can be overlap of the vortex cores and there can be an attractive interaction between vortices. This effect was established experimentally by Essmann and Trauble (22) with experiments in which they decorated the surface of Nb with Fe spheres about 4 nm in diameter. To perform these experiments, typically an array of vortices is trapped in a coin-shaped Nb sample by applying a magnetic field above H_{c1} and then turning the field off. A "smoke" of Fe was then created by evaporating Fe metal in an atmosphere of a few Torr of He gas. The tiny Fe particles that are created follow the flux lines to the point on the surface where the core of the vortex emerges. Once the Fe particles touch the Nb, they stick very strongly. To image the vortex lattice, the Fe is stripped off the surface by a graphite replication technique and viewed in a transmission electron microscope. For the initial flux entry in the first-order transition of H_{c1}, illustrated by the dashed curve of Fig. 6, it is found that there is a two-phase region. There are clusters of a few hundred vortices all on a triangular lattice and separated by about 200 nm. Between these clusters there are Meissner-like or vortex-free regions. In this two-phase region, the spacing of the vortices is independent of magnetic field. As the magnetic field increases, the sample fills with vortices having 200 nm spacing. The magnetization curve in this region is linear with a slope governed by the demagnetizing factor. An abrupt change in the slope of the magnetization curve occurs when the sample is just filled with vortices at the lattice spacing governed by the attractive interaction between vortices. This characteristic field is denoted by B_0. At higher magnetic fields, the vortices are pushed closer together and the magnetization curve is similar to the repulsive force case for high-κ materials. Auer and Ullmaier (7) performed a very systematic study of these same effects, as κ in Ta is systematically increased from type I to type II behavior by alloying with N.

To analyze quantitatively the transition from type I to type II behavior by alloying, it is useful to focus on the connection between the coherence distance and the normal-state electronic mean free path l. With small additions of impurity, ξ is given by

$$1/\xi \approx 1/\xi_0 + 1/\ell \qquad (19)$$

where ξ_0 is the intrinsic or clean limit of ξ. At higher impurity concentrations, l becomes comparable to ξ_0 and the diffusion limit is more appropriate. In this regime

$$\xi = \sqrt{\xi_0 \ell} \qquad (20)$$

Experiments to Determine H_{c1} and H_{c2}

Many factors can lead to errors in determining both H_{c1} and H_{c2}. The lowest field for which a vortex is thermodynamically stable in a superconductor is defined to be H_{c1}. It is a difficult quantity to measure because thermodynamic equilibrium is not achieved easily at fields close to H_{c1}. The most common error arises from the presence of surface barriers to flux entry into the sample. For a cylindrical superconductor with a radius of curvature much larger than both λ and ξ (17, p. 79), the applied field must be larger than H_{c1} before a vortex will nucleate. As the field increases from zero, Meissner screening currents flow in the superconductor within a distance λ of the surface. When a vortex starts to nucleate at the surface and move into the interior of the sample, an image vortex develops to pull the vortex back toward the surface. The competition between the image force pulling the vortex toward the surface and the Meissner currents pushing the vortex into the interior creates a surface barrier to flux entry. Often the flux-entry field is comparable to H_c. To overcome this effect, the surface needs to be rough on the scale of the penetration depth or the surface needs to be coated in some way to suppress the surface barrier to zero.

The highest field for which a vortex is thermodynamically stable in a superconductor is defined to be H_{c2}. For a sample that obeys the Ginzburg-Landau theory, there is a sharp change in slope at the second-order phase transition of a reversible magnetization curve that identifies H_{c2}. This is the most reliable measurement of H_{c2}. Measurements of the electrical resistivity is less reliable because it depends on the motion or depinning of vortices and often is not a measure of the point of thermodynamic stability of a vortex. For a clean classical superconductor such as Nb, the electrical resistance goes to zero at very nearly the same field that the magnetization goes linearly to zero, and both resistivity and magnetization methods can be used to determine H_{c2}. For high-T_c materials, the situation is more complicated. Because ξ is so small, fluctuation effects smear out the normal-metal to superconductor transition so that is is typically 3 K wide. Both the magnetization curves and the electrical resistivity are greatly rounded even for a very perfect sample. For this case, it is better to move to lower fields at which fluctuations are negligible and use a fit of the M vs H data to the Hao–Clem theory to determine H_{c2}.

BIBLIOGRAPHY

1. D. L. Decker, D. E. Mapother, and R. W. Shaw, Critical field measurements on superconducting lead isotopes, *Phys. Rev.,* **112**: 1888–1897, 1958.
2. G. Bednorz and K. A. Muller, Possible high T_c superconductivity in the Ba-La-Cu system, *Z. Phys. B,* **64**: 189–197, 1986.
3. D. K. Finnemore and D. E. Mapother, Superconducting properties of tin, indium, and mercury below 1 K, *Phys. Rev.,* **140**: A507–A518, 1965.
4. R. B. Goldfarb, Demagnetizing factors. In J. Evetts (ed.), *Concise Encyclopedia of Magnetic and Superconducting Materials,* Oxford: Pergamon, 1992.
5. D. Shoenberg, *Superconductivity,* Cambridge: Cambridge University Press, 1960.
6. M. Tinkham, *Introduction to Superconductivity,* 2nd ed., New York: McGraw-Hill, 1996.
7. J. Auer and H. Ullmaier, Magnetic behavior of type II superconductors with small Ginsburg-Landau parameter, *Phys. Rev.,* **7**: 136–145, 1973.
8. D. K. Finnemore, T. F. Stromberg, and C. A. Swenson, Superconducting properties of high purity Nb, *Phys. Rev.,* **149**: 231–243, 1966.
9. J. J. Wollan et al., Phase transition at H_{c1} for superconducting Nb and V, *Phys. Rev.,* **10**: 1874–1880, 1974.
10. U. Kumpf, Magnetization curves for type II superconductors with small Ginsburg-Landau parameter, *Phys. Status Solidi,* **44**: 829–843, 1971.
11. R. R. Hake, Mixed state paramagnetism in high field type II superconductors, *Phys. Rev. Lett.,* **15**: 865–868, 1965.
12. J. Bardeen, L. N. Cooper, and J. R. Schrieffler, Theory of superconductivity, *Phys. Rev.,* **108**: 1175–1204, 1957.
13. L. N. Cooper, Bound electron pairs in a degenerate Fermi gas, *Phys. Rev.,* **104**: 1189–1190, 1956.
14. F. London, *Superfluids,* New York: Wiley, 1950, Vol. 1.
15. V. L. Ginzburg and L. D. Landau, Regarding a theory of superconductivity, *Zh. Expt. Teor. Fiz.,* **20**: 1064–1072, 1950; **20**: 1064–1077, 1950.
16. A. L. Fetter and P. C. Hohenberg, Theory of type II superconductors. In R. D. Parks (ed.), *Superconductivity,* Marcel Dekker: New York, 1969.
17. P. G. de Gennes, *Superconductivity of Metals and Alloys,* New York: W. A. Benjamin, 1966.
18. A. A. Abrikosov, Magnetic properties of superconductors, *Zh. Expt. Teor. Fiz.,* **32**: 1442–1450, 1957 (*Sov. Phys. JETP,* **5**: 1174–1182, 1957).
19. Z. Hao and J. R. Clem, Limitations of the London model for the reversible magnetization of type II superconductors, *Phys. Rev. Lett.,* **67**: 2371–2373, 1991.
20. J. Sok et al., Reversible magnetization, critical fields, and vortex structure in grain aligned $YBa_2Cu_4O_8$, *Phys. Rev.,* **51**: 6035–6040, 1992.
21. J. E. Ostenson, J. R. Hopkins, and D. K. Finnemore, Surface superconductivity in Nb and V, *Physica,* **55**: 502–506, 1971.
22. U. Essmann and H. Trauble, Direct observation of individual flux lines in type II superconductors, *Phys. Lett.,* **A24**: 526–527, 1967.

D. K. FINNEMORE
Iowa State University

SUPERLATTICES, MAGNETIC. See MAGNETIC EPITAXIAL LAYERS.

SUPPLY AND DEMAND SIDE MANAGEMENT. See LOAD MANAGEMENT.